Research Article

Bearing Response Prediction in Hydrothermal Aged Carbon Fiber Reinforced Epoxy Composite Joints Using Machine Learning Techniques

Mohit Kumar [a]* , **Govind Vashishtha [b]** , **Babita Dhiman [c]** , **Sumika Chauhan [b]**

[a] Department of Mechanical Engineering, Chandigarh University, Mohali, Punjab, 140301, India

[b] Faculty of Geoengineering, Mining and Geology, Wroclaw University of Science and Technology, Na Grobli 15, 50-421 Wroclaw, Poland
[c] Department of Electronics and Communication Engineering, Chandigarh University, Mohali, Punjab, 140301, India

ABSTRACT

Keywords:

Carbon Fiber;
Epoxy resin;
Machine Learning;
Bearing Response;
Support vector regression.

The work focuses on predicting the bearing response in hydrothermal-aged carbon fiber-reinforced epoxy composite (CFREC) joints through the utilization of machine learning techniques. CFREC are extensively employed in aerospace and other high-performance applications, and their long-term structural integrity is of paramount importance. The hydrothermal aging process can significantly affect the mechanical behavior of such composites, particularly in joint configurations. In this research, an innovative support vector regression approach is present that leverages machine learning algorithms to forecast the bearing response of CFREC joints after undergoing hydrothermal aging. The study encompasses the development of predictive models using a comprehensive dataset of experimental observations. The machine learning technique, support vector regression is trained and evaluated to assess their accuracy and reliability in predicting bearing response. The results show that the overall percent reduction in bearing response, after 30 days of pristine composite bolted joints at 0 Nm bolt torque shows reductions of 23.22 % at 65℃, respectively. Conversely, under the same conditions, MWCNTs added composite bolted joints exhibit only a 9.2% reduction. The predictive models find the value of 0.0081 RSME and 0.8 R2 respectively through support vector regression confirming that the predicted values lie in between the upper and lower bond.

1. Introduction

In the ever-evolving landscape of advanced materials and structural engineering, the durability and performance of composite structures remain a pivotal focus. Carbon fiber reinforced epoxy composites (CFREC) have garnered significant attention for their exceptional mechanical and corrosion resistance properties. These composites are generally manufactured using thermal curing techniques for many years but the disadvantage of several hours of processing time unlocks the potential of other curing techniques i.e., radiation curing. To cure CFREC composites, several out-of-autoclave curing methods have been suggested, including ultraviolet (UV) technology, X-rays, gamma rays, and electron beam (EB) technology. Amid these curing processes, EB curing stands out as a state-of-the-art technology for polymer-based composite materials. Its noteworthy features include high controllability, environmental friendliness, high curing efficiency, room temperature curing, rapid curing time, low energy consumption, and cost-effectiveness. So, the benefits of the EB curing technique enable the

---

* Corresponding author.
E-mail address: mohit.dhiman349@gmail.com

development of CFREC-based structural components. These structural components are made of joints that can be mechanical or adhesive. These composite structural joints are subjected to aging environments in a variety of applications in the civil and marine industries. So, understanding their behavior under realistic environmental conditions, such as hydrothermal aging, is critical for ensuring long-term structural integrity [1-4]. The significance of environmental elements, including temperature and humidity, on the structural functionality of CFREC joints should not be underestimated. The absorption of moisture in composites diminishes their mechanical, thermal, physical, electrical, and chemical characteristics. Physical alterations and chain scission induce plasticization and swelling in epoxy, while hydrolysis results from chemical transformations [5-6]. FRP composite deterioration is reliant on the durability of the fiber-polymer contact and its integral phases [7-8]. However, swelling diminishes interface strength, which has an impact on the mechanical properties of composites. Altogether, moisture absorption diminishes mechanical properties, lowers glass transition temperatures, causes polymer swelling, and enhances the viscoelasticity of FRP composites [9–11]. As a result, the strength retention of structural composites in hydrothermal circumstances is a significant problem for companies and academics.

The literature available investigated the behavior of FRP composites under hydrothermal aging conditions. Alessi et al. [12] studied the water-absorption behavior in carbon/epoxy composites at temperatures of 30°C and 70°C, for 30 and 60 days, respectively. Hong et al. [13] investigated the durability of submerged CFREC in water at temperatures of 23 °C, 40 °C, and 60 °C, respectively. Even with the useful insights provided by the aforementioned studies, they are limited to certain material qualities and experiment settings and can't fully define the role of other elements. Furthermore, experimental studies of various factors are often time-consuming and ineffective. To save time and effort while covering as many parameters as possible, the Machine learning approach is utilized in FRP composites.

Machine learning (ML) approaches can translate feature representations to composite mechanical properties [14–18]. However, a survey of the literature reveals that there have been few attempts to construct a complete prediction approach to characterize the mechanical response. Machello et al. [19] conducted a thorough examination of the capabilities of ML algorithms in addressing the limitations of traditional models for forecasting

the durability of FRP composites. Alhusban et al. [20] evaluated the existing utilization of different ML algorithms in reinforcing Reinforced Concrete (RC) members with FRP. This assessment aimed to enable researchers to gauge the effectiveness of current approaches and pinpoint areas for further investigation, with the goal of bridging knowledge and practice gaps. The search for relevant literature involved querying Scopus databases based on predefined criteria. However, However, despite their impressive capabilities, these techniques face several challenges and limitations that can impact their effectiveness. One of the primary challenges is the quality and quantity of data; machine learning models require vast amounts of high-quality data to achieve accurate predictions, and insufficient or noisy data can significantly degrade performance. Additionally, the issue of overfitting, where a model learns the training data too well but fails to generalize to new, unseen data, poses a critical limitation.

There have been very few attempts to examine the ML approach to predict the bearing response of CFREC joints under hydrothermal aging. The novelty of our research lies in its dual focus on both hydrothermal aging and predictive modeling. By incorporating SVM, a method proven effective in various engineering applications, the aim is to provide a broad understanding of how aging impacts the bearing capacity of CFREC joints. The outcomes of this study hold the potential to guide future advancements in both material science and machine learning applications for structural engineering, ensuring the continued evolution of resilient and sustainable composite structures in real-world conditions.

2. Materials and Methods

The subsequent section comprehensively addresses the acquisition of materials, fabrication of composite laminates, and execution of essential tests pertinent to the ongoing research.

2.1. Materials

In this work, a matrix of thermoset epoxy resin bisphenol A and a reinforcement of 200 GSM woven carbon fabric were employed. The cationic-photoinitiator used, bis(4-methylphenyl) iodonium hexafluorophosphate, was sourced from Sigma-Aldrich in Missouri, USA. Upon exposure to EB rays, this initiator decomposes into protonic acid H+ which then reacts with the epoxy group's oxygen (O_2). Additionally, multi-walled carbon nanotubes (MWCNTs) were incorporated as nanofillers to enhance the strength properties of the

composite. The material specifications are given in Table 1.

2.2. Preparation of EB Cured CFREC

The manufacturing process of EB-cured CFREC involves three key steps: hand-layup method, exposure to EB radiations, and post-curing [21]. This method allows for the creation of two distinct materials: pristine CFREC laminates and CFREC/MWCNTs composites. To begin, 0.3 wt.% of MWCNTs were added to 120 ml of acetone and mechanically agitated for 30 minutes at 6000 rpm using a homogenizer. Subsequently, the mixture was ultra-sonicated for 60 minutes using a Q-Sonica probe sonicator (40Hz, 700W).

Table 1. Material Specification

Materials	Properties	Value
Carbon Fabric (200 GSM, Woven)	Tensile strength	4000 Mpa
	Tensile modulus	240 GPa
	Elongation	1.7 %
	Density	1.8 g/cm^3
	Areal weight	200 g/m^2
	Poisson ratio	0.3
Epoxy Resin, L-12	Density	1.15g/cm^3
	Viscosity	11000mPa
Bis(4-methyl-phenyl) iodonium-hexafluoro-phosphate	Pure	98 %
	Melting temperature	175-180°C
Multiwalled carbon nanotubes (NC 7000)	Average length	1.5 µm
	Average diameter	9.5 nm
	Carbon purity	90%
	Surface area	275 m^2/g

Next, a cationic initiator, specifically bis(4-methylphenyl) iodonium hexafluoro-phosphate, was dissolved in acetone at a concentration of 2 wt.% using a sonication technique. This initiator solution is then added to a premeasured quantity of epoxy. The epoxy-initiator mixture is combined with the MWCNTs/acetone suspension and agitated at 60°C and 9000 rpm until the acetone is completely evaporated. This process ensures thorough dispersion of the MWCNTs within the epoxy matrix, facilitating uniform properties all over. Weighing the mixture both before and after the treatment guaranteed that all of the acetone had been removed. After a 30-minute sonication process, the epoxy/MWCNTs/ initiator suspension underwent preparation for composite laminate production using a hand layup technique. The composite laminate was formed by combining the final suspension with woven carbon fabric, utilizing a stacking

sequence of [0/90]6. To facilitate the curing process, the laminates were enclosed within aluminum molds, and a releasing gel was applied to prevent adhesion. To ensure uniform thickness, continuous pressure was applied through clamps positioned on the mold's sides. Subsequently, the molds were subjected to the electron beam (EB) curing process at the Bhabha Atomic Research Centre (BARC) in Mumbai, India, utilizing a 4 MeV pulsed horizontal accelerator machine (refer to Fig. 1). The EB curing process involved maintaining a pulse current of 100 mA, a frequency of 10 Hz, and a conveyor speed of 3 cm/sec. A total irradiation dose of 240 kGy was administered at a dose rate of 10 kGy/pass. Following EB irradiation, the laminates underwent post-curing at 100°C for two hours. The resulting EB-cured CFREC/MWCNTs laminate exhibited an ultimate thickness of 2 ± 0.2 mm. Similarly, EB-cured pristine CFREC laminates were produced using identical production processes. Figure 2 displays FESEM images of the prepared MWCNTs added composites.

## 2.3. Preparation of CFREC Joints

For bearing responses, the joints were built using pristine and MWCNTs added CFREC laminates following ASTM D5961. As per this standard, the geometric parameters E/D and W/D are taken as 5 and 6. The M4 size shoulder bolt was inserted through a hole with a diameter of 4 mm. The automated drilling machine precisely drilled the bolt hole, ensuring consistency among all specimens with a tolerance of ±0.05 mm, as per ASTM D5961 standards. **Figure 3** illustrates a schematic diagram of the CFREC joint and fixture.

2.4. Hygrothermal Aging Condition

For hydrothermal aging, the prepared CFREC joint specimens were provided with three different temperatures in digitalized water bath MSW-273(SL), MAC *i.e.,* 25°C, 45°C, and 65°C for 30 days. The specimens were carried out of a water-bath at different time intervals (10, 20, and 30 days) and dried with tissue paper before being weighed on a high-precision weight machine with a precision of 0.0001 g.
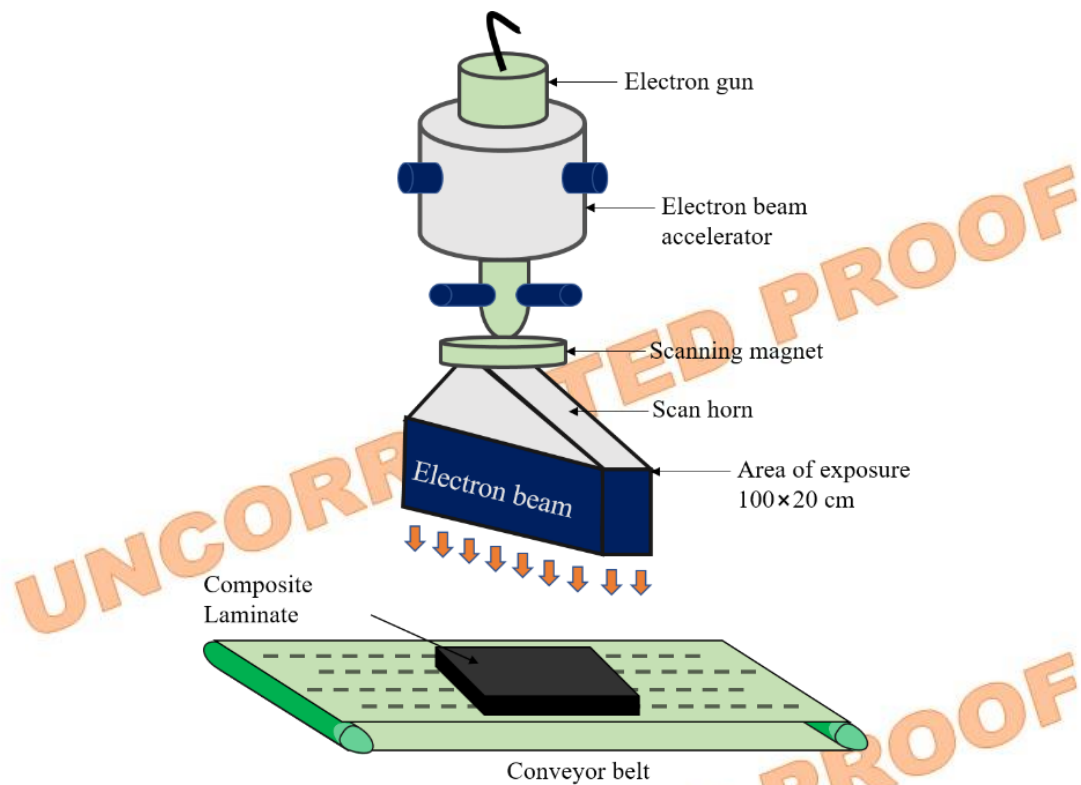
Fig. 1. Setup of pulsed electron beam accelerator
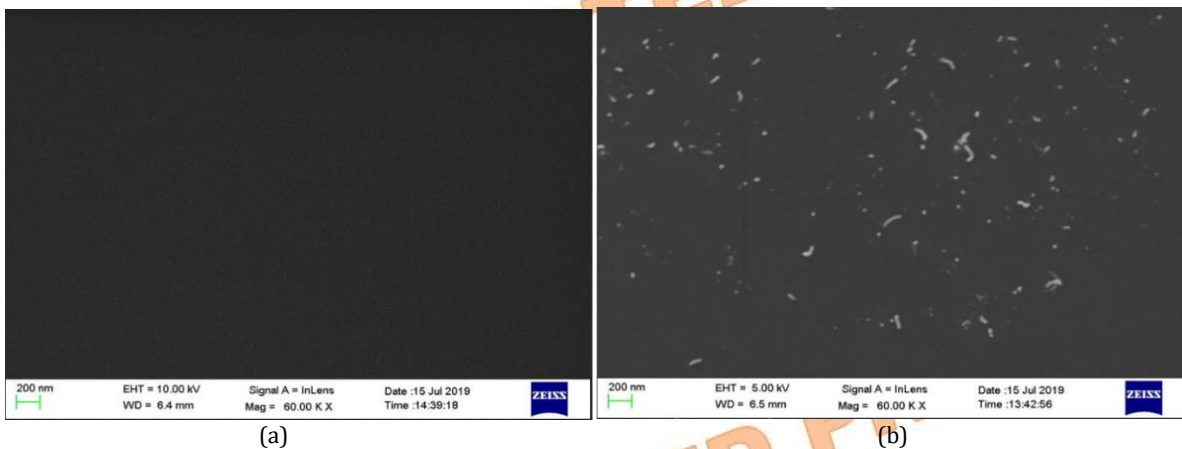
Fig. 2. FESEM of (a) pristine CFREC and (b) 0.3 wt.% added MWCNTs in CFREC sample

2.5. Machine Learning Approach

2.5.1. Support Vector Regression (SVR)

In the proposed work, the support vector regression (SVR) has been used as a machine learning technique. In addition to Support Vector Machines (SVM), various other machine learning techniques can be utilized for predictive studies, including decision trees, random forests, neural networks, k-nearest neighbors (k-NN), gradient boosting machines (GBM), and logistic regression. Each method has its strengths, such as the simplicity and interpretability of decision trees, the ensemble power of random forests and GBM, and the flexibility and high performance of neural networks for complex data. SVM is often used in predictive studies due to its effectiveness in high-dimensional spaces, robust handling of outliers, and ability to create a clear margin of separation between classes. It is particularly well-suited for classification tasks with a relatively small to medium-sized dataset and where the decision boundary is not necessarily linear.
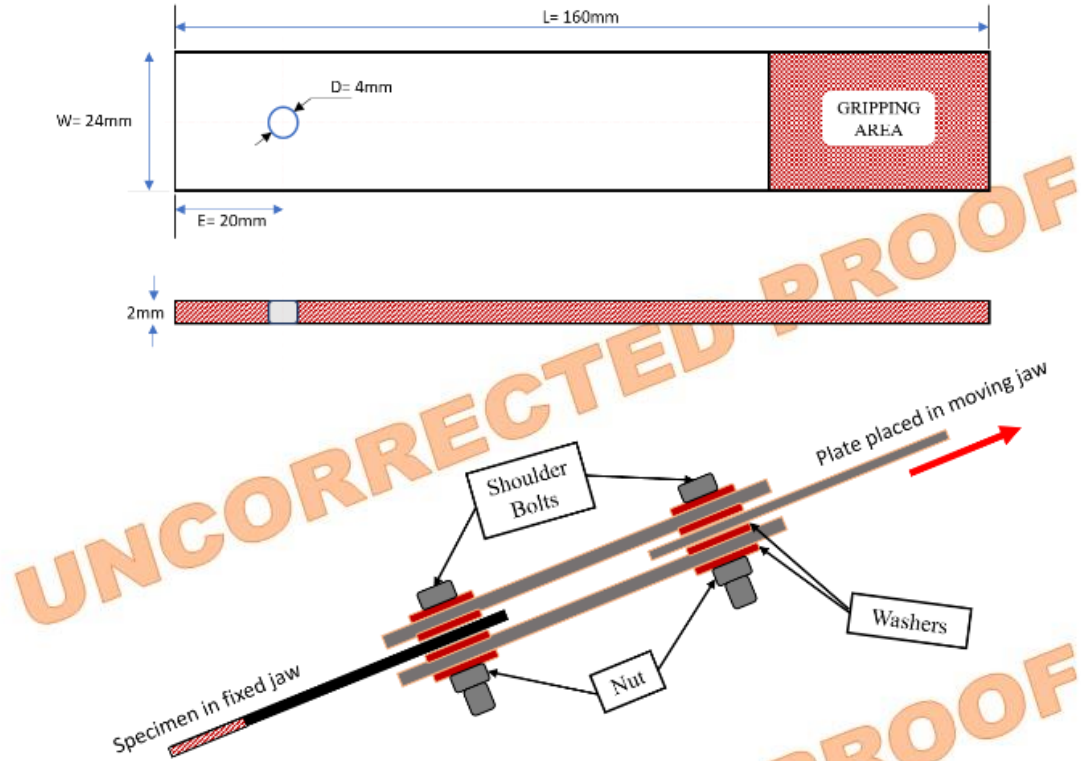
4

Fig. 3. Schematic diagram of CFREC joint and fixture

Vapnik pioneered the application of the supervised learning method, specifically Support Vector Machines (SVM), for data classification. The utilization of a hyperplane is a key aspect in categorizing the training data within a two-dimensional space, as shown in Fig. 4.

In N number of data (x_i, y_i), where $i = 1\ to\ N$, the x_i signifies the input data and $y_i \in \{-1,1\}$ symbolizes the class. SVM determines the optimum hyperplane by maximizing the margin amid different classes. This hyperplane is positioned to achieve the greatest separation between the hyperplane itself and the closest point within every class.

$$Minimize\ \frac{1}{2}\|w\|^2 + C\sum_{i=1}^{n}\xi_i \qquad (1)$$

Subjected to $y_i(w^T x_i + b) \geq 1 - \xi_i$ and $\xi_i \geq 0\ for\ i = 1\ to\ N$,

In the equations, the variables $w, \xi_i, T,\ and\ b$ denote the weight vector, slack variable, transpose, and bias. The values of w and b are determined through the training method. The regularization constraint C plays a crucial role in controlling the model's complexity by striking a balance among margins. The Lagrange multiplier α_i gives the hyperplane as a quadratic and incorporates constraints in a quadratic equation, transforming them into unconstrained conditions. The factor w is sourced from Refs.

[22-23]. The SVM's objective function is formally definite in Eq. (2).

$$w(\alpha) = \sum_{i=1}^{n}\alpha_i + \frac{1}{2}\sum_{i,j=1}^{n}\alpha_i\,\alpha_j x_i y_i k(x_i, x_j) \qquad (2)$$

where, α_i, α_j implies the Lagrange multiplier and $k(x_i, x_j)$ as the kernel function.

$$f = sign(b + \sum_{SV}[(\alpha_i y_i)k(x_i, x_j)]) \qquad (3)$$

In the case of the Lagrange multiplier, SV functions as a supporting vector. The assessment of dot product in feature space necessitates the transformation of input statistics into feature space, a task efficiently carried out by the kernel function. **Table 2** enumerates several widely used kernel functions, showcasing their popularity in diverse applications.
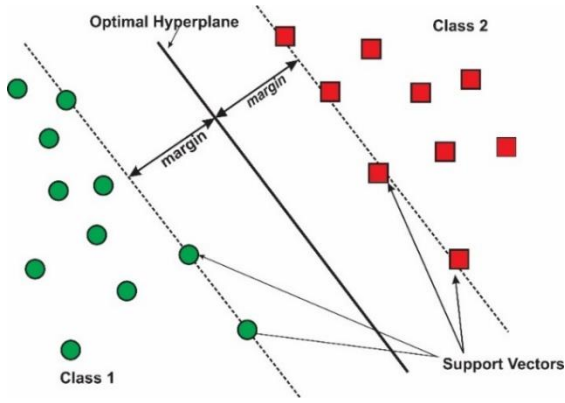
5

Fig. 4. Basic architecture of SVM

Table 2. Different kernel function

Kernel-function	Column C
Linear function	$k(x_i, x_j) = x_i.x_j$
Polynomial function	$(x_i, x_j) = (\gamma x_i.x_j + r)^d, \gamma > 0$
Radian basis function (RBF)	$k(x_i, x_j) = \exp(-\gamma \|x_i - x_j\|^2), \gamma > 0$
Sigmoid function	$k(x_i, x_j) = tanh(\gamma x_i.x_j + r)$

2.5.2. SVM Parameters

The enactment of SVM is significantly influenced by two key parameters: the regularization parameters (C) and the kernel parameters (γ). Choosing the right value for parameter C is essential because it minimizes misclassification by maximizing the margin and decreasing training error. A higher C value leads to lower bias but risks overfitting, while a smaller C value may result in higher bias and lower variance, causing underfitting. Hence, careful consideration is necessary for an optimal C selection. In the present work, the radian basis γ is employed to convert input data into a higher-dimensional space, controlling the peaks. The small γ value produces sharp peaks, whereas a higher γ value generates softer peaks. The judicious choice of these parameters is essential for achieving accurate predictions. The implementation of an inbuilt optimization algorithm, specifically Bayes optimization in MATLAB, has facilitated this work.

2.6. Performance Measures

R² score error: The R² square shows a dynamic role in validating the robustness of the model whose mathematical formulation is given in Eq. (4). This parameter indicates how closely the predicted value matches the actual data and varies between 0 and 1. In this measure, the

independent variables are preferred for constructing the accurate model.

$$R^2 = \frac{\sum_{i=1}^{n}(\hat{y}_i - y_i)^2}{\sum_{i=1}^{n}(y_i - \bar{y}_i)^2} \tag{4}$$

where n represents the data points, y_i represents the observed values, $\hat{y}_i$ indicates the predicted values and $\bar{y}_i$ represents the mean of y_i.

Median absolute error (MAE): This statistical parameter measures the average of absolute error among the predicted and actual values. The mathematical formulation of the MAE is given in Eq. (5).

$$MAE = \sum_{i=1}^{n} \frac{(\hat{y}_i - y_i)}{n} \tag{5}$$

Mean squared error (MSE): This is computed by taking the square of the deviation error and then determining the average of it. The values of MSE vary in the range of zero to infinity, therefore small values are desirable. The mathematical formulation of MSE is shown in Eq. (6).

$$MSE = \frac{1}{n}\sum_{i=1}^{n}(y_i - \hat{y}_i)^2 \tag{6}$$

Root Mean squared error (RMSE): This resembles the MSE, the difference lies in the square root. RMSE ranges from zero to infinity, but smaller RMSE values are typically preferred. Equation (7) provides the formula for RMSE.

$$RMSE = \sqrt{\sum_{i=1}^{n} \frac{(y_i - \hat{y}_i)^2}{n}} \tag{7}$$

3. Methodology

The proposed methodology has been implemented on Matlab software. The SVM/SVR is used for classification, clustering, and regression analysis. It is a supervised learning algorithm. In the proposed methodology the SVR is implemented to predict the bearing strength of the CFREC joints hydrographic bolts under hydrothermal aging conditions. The methodology flowchart is shown in the **Fig. 5.**

4. Results and Discussion

4.1. Results From Traditional Approach

Under a hydrothermal aging environment, the performance of CFREC joints was investigated. After conditioning, these joint specimens were fastened into a fixture (**Fig. 3**). Before testing, the composite joints were tightened with 3 bolt tightening torques- 0, 2, and 4Nm. The tightened bolt torque was measured with a standardized torque wrench. These joint specimens were then

tested on a UTM machine, Zwick Roell, with 10 kN capacity and 2 mm/min crosshead speed. **Figure 6** depicts the bearing response of unaged EB-cured CFREC specimens in pristine and MWCNTs added configurations at different bolt torques. The zigzag pattern on the graph represents the bearing mode of failure.
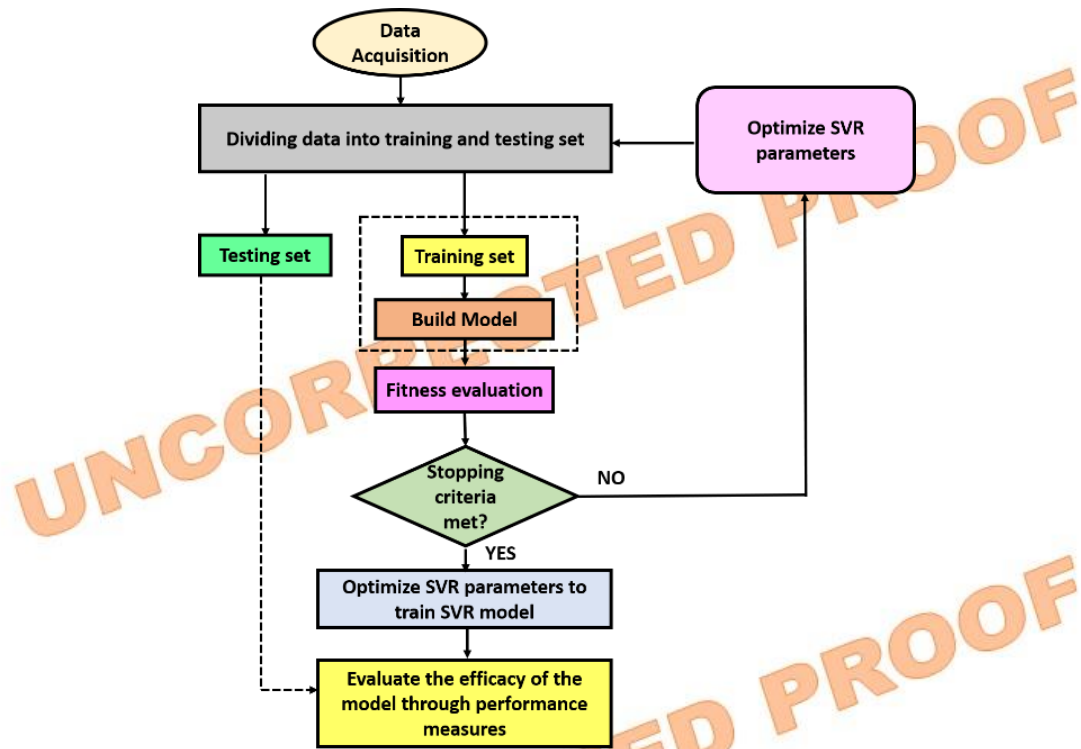

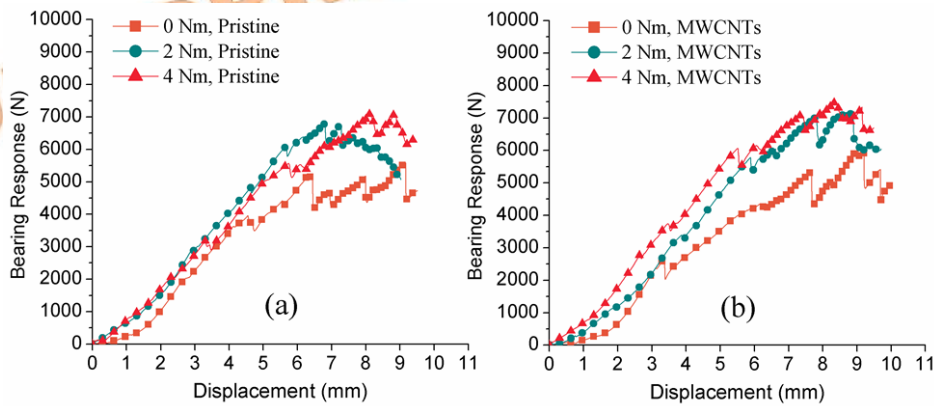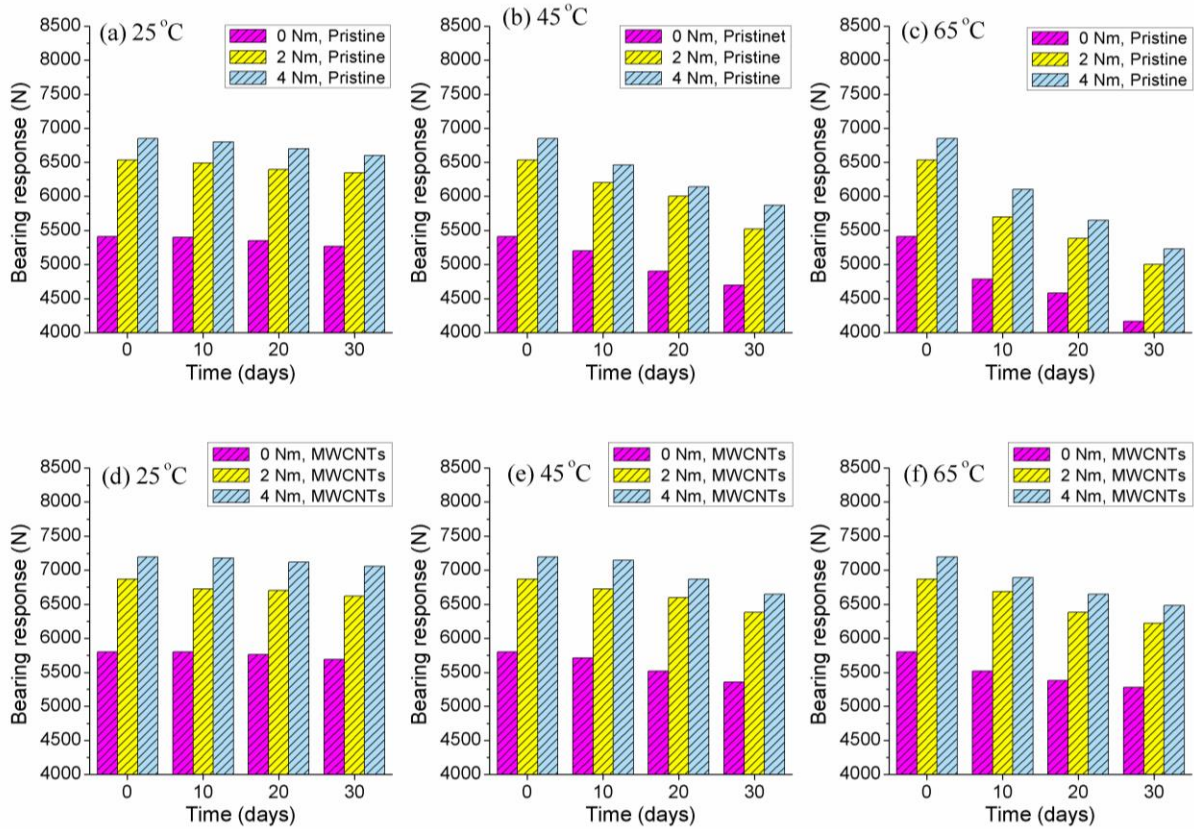**Fig. 5.** Flowchart of proposed methodology

Fig. 6. Bearing response of unaged CFREC joint specimens

In Fig. 7, a bar graph illustrates the comparison between pristine and MWCNTs-infused CFREC joint specimens with and without aging conditions, with variable bolt torques.

Fig. 7. Bearing response of aged CFREC joint specimens at different bolt torque

The results indicate a higher bearing response in MWCNT joint specimens compared to pristine ones. This enhancement is ascribed to the development of robust MWCNTs/epoxy interfacial bonds and exceptional barrier properties, that mitigate interfacial debonding during aging [24-25]. In contrast, pristine joint specimens experience a deteriorating effect on bearing response because of prolonged water exposure and elevated temperatures. The degradation becomes more pronounced with increasing temperature and duration, leading to a significant reduction in bearing response after 30 days of aging. Elevated water temperatures contribute to increased polymeric chain movement, accelerating water absorption and compromising the enactment of composite bolted joints. Pristine configurations exhibit higher water absorption rates, causing epoxy swelling and microcrack formation at the fiber-matrix interface, further contributing to joint deprivation. In contrast, the inclusion of MWCNTs lowers water absorption rates, even at higher temperatures, because of tortuosity generation, interfacial bonds, and enhanced barrier properties. The graph in Fig. 7 also demonstrates the positive influence of bolt torques in hydrothermal conditions. Comparing the overall percent reduction in bearing response, after 30 days pristine composite bolted joints at 0 Nm bolt torque show reductions of 4.45 %, 14.33 %, and 23.22 % at 25°C, 45°C, and 65°C, respectively. Conversely, MWCNTs added composite bolted joints exhibit lower reductions of 2.50 %, 7.01 %, and 9.23 % at the same temperature conditions and duration.

4.2. Results from Machine Learning Approach

The proposed methodology has been carried out to predict the bearing strength of the bolt after hydrothermal aging. These 27 experimental runs have been conducted. Out of which 80% have been utilized to train the model whereas the remaining statistics are used for testing and validation. The predicted results have been evaluated on the above statistical parameters. The evaluated statistical parameters are shown through a bar plot as shown in **Fig. 8. Figure 8** shows that predicted values obtained by the proposed methodology are close to actual values as values for the statistical analysis are approaching their optimum values. The predicted values obtained by the SVR are shown in **Fig. 9**. At a 95% confidence level, the predicted values have also been plotted by the SVR as shown in **Fig. 10**. From **Fig. 9-10,** it is validated that predicted values lie within the upper and lower bounds.
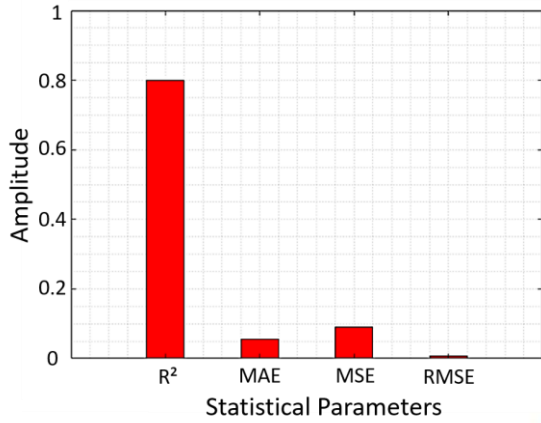
8

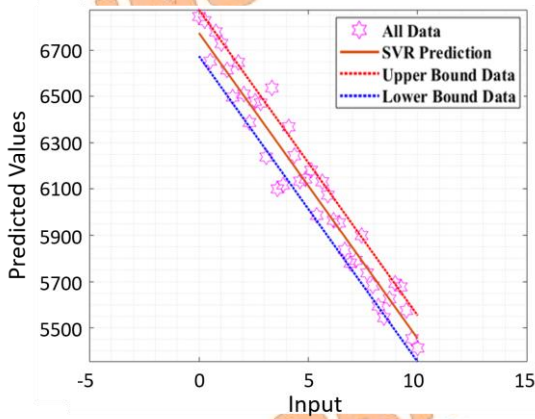**Fig. 8.** Predicted results of statistical parameters

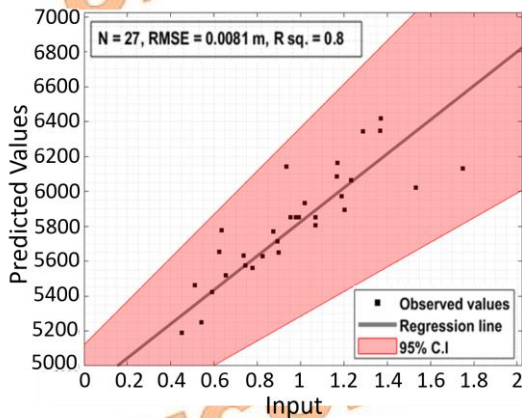**Fig. 9.** Predicted results obtained by SVR

Fig. 10. Predicted results obtained by SVR at 95% confidence level

5. Conclusions

Our research is unique in its simultaneous exploration of hydrothermal aging and predictive modeling. Utilizing the well-established SVM method has demonstrated the effective influence of aging on the bearing capacity of CFREC joints.

The following conclusion has been drawn from the present work:

- The overall percent reduction in bearing response, after 30 days of pristine composite bolted joints at 0 Nm bolt torque show reductions of 4.45 %, 14.33 %, and 23.22 % at 25°C, 45°C and 65°C, respectively. Conversely, MWCNTs added composite bolted joints exhibit lower reductions of 2.5%, 7.0%, and 9.2% at the same temperature conditions and duration.
- The addition of MWCNTs increases the bearing strength retention by up to 90% as compared to pristine specimens having 76% strength retention under the same conditions.
- The results of the conventional experimentation are validated through the machine learning approach. The value of 0.0081 RSME and 0.8 R^2 respectively has been obtained through support vector regression. The predicted values lie in between the upper and lower bonds.

6. Future scope

In the future, authors can utilize the more robust machine learning approach such as LSTM and CNN to get better results.

Conflicts of Interest

The author declares that there is no conflict of interest regarding the publication of this article.

References

[1] Palaniappan, S.K., Singh, M.K., Rangappa, S.M. and Siengchin, S., 2023. Eco-friendly Biocomposites: A Step Towards Achieving Sustainable Development Goals. *Composites*, *7*(12), pp. 7373.

[2] Kumar, M, Saini, J.S. and Bhunia, H., 2020. Performance of mechanical joints prepared from carbon-fiber-reinforced polymer nanocomposites under accelerated environmental aging. *Journal of Materials Engineering and Performance* 29, pp. 7511-7525.

[3] Kumar, M., Saini, J.S., Bhunia, H. and Chowdhury, S.R., 2021. The behavior of mechanical joints prepared from EB-cured

CFRP nanocomposites subjected to hygrothermal aging under bolt preloads. *Applied Composite Materials*, *28*, pp.271-296.

[4] Dhiman, N., Saini, J.S. and Kumar, M., 2023. Hygrothermal effect on strength of thermally cured glass epoxy nanocomposite made joints. *Proceedings of the Institution of Mechanical Engineers, Part C: Journal of Mechanical Engineering Science*, *237*(23), pp.5692-5707.

[5] [2] De'Nève, B. and Shanahan, M.E.R., 1993. Water absorption by an epoxy resin and its effect on the mechanical properties and infra-red spectra. *Polymer*, *34*(24), pp. 5099-5105.

[6] [3] Zheng, Q. and Morgan, R.J., 1993. Synergistic thermal-moisture damage mechanisms of epoxies and their carbon fiber composites. *Journal of Composite Materials*, *27*(15), pp. 1465-1478.

[7] [4] Ray, B.C., 2006. Temperature effect during humid ageing on interfaces of glass and carbon fibers reinforced epoxy composites. *Journal of colloid and interface science*, *298*(1), pp. 111-117.

[8] [5] Suyambulingam, I., Rangappa, S.M. and Siengchin, S., 2023. Advanced Materials and Technologies for Engineering Applications. *Applied Science and Engineering Progress*, *16*(3), pp. 6760-6760.

[9] [6] Tian, W. and Hodgkin, J., 2010. Long-term aging in a commercial aerospace composite sample: Chemical and physical changes. *Journal of Applied Polymer Science*, *115*(5), pp. 2981-2985.

[10] [7] Dao, B., Hodgkin, J.H., Krstina, J., Mardel, J. and Tian, W., 2007. Accelerated ageing versus realistic ageing in aerospace composite materials. IV. Hot/wet ageing effects in a low temperature cure epoxy composite. *Journal of applied polymer science*, *106*(6), pp. 4264-4276.

[11] [8] Dao, B., Hodgkin, J., Krstina, J., Mardel, J. and Tian, W., 2010. Accelerated aging versus realistic aging in aerospace composite materials. V. The effects of hot/wet aging in a structural epoxy composite. *Journal of applied polymer science*, *115*(2), pp. 901-910.

[12] [9] Alessi, S., Pitarresi, G. and Spadaro, G., 2014. Effect of hydrothermal ageing on the thermal and delamination fracture behaviour of CFRP composites. *Composites Part B: Engineering*, *67*, pp. 145-153.

[13] [10] Hong, B., Xian, G. and Wang, Z., 2018. Durability study of pultruded carbon fiber reinforced polymer plates subjected to water immersion. *Advances in Structural Engineering*, *21*(4), pp. 571-579.

[14] [11] Yin, B.B. and Liew, K.M., 2021. Machine learning and materials informatics approaches for evaluating the interfacial properties of fiber-reinforced composites. *Composite Structures*, *273*, pp. 114328.

[15] [12] Naser, M.Z., Thai, S. and Thai, H.T., 2021. Evaluating structural response of concrete-filled steel tubular columns through machine learning. *Journal of Building Engineering*, *34*, pp. 101888.

[16] [13] Chaabene, W.B., Flah, M. and Nehdi, M.L., 2020. Machine learning prediction of mechanical properties of concrete: Critical review. *Construction and Building Materials*, *260*, pp. 119889.

[17] [14] Ford, E., Maneparambil, K., Rajan, S. and Neithalath, N., 2021. Machine learning-based accelerated property prediction of two-phase materials using microstructural descriptors and finite element analysis. *Computational Materials Science*, *191*, pp. 110328.

[18] [15] Sacco, C., Radwan, A.B., Anderson, A., Harik, R. and Gregory, E., 2020. Machine learning in composites manufacturing: A case study of Automated Fiber Placement inspection. *Composite Structures*, *250*, pp. 112514.

[19] [16] Machello, C., Bazli, M., Rajabipour, A., Rad, H.M., Arashpour, M. and Hadigheh, A., 2023. Using machine learning to predict the long-term performance of fibre-reinforced polymer structures: A state-of-the-art review. *Construction and Building Materials*, *408*, pp. 133692.

[20] [17] Alhusban, M., Alhusban, M. and Alkhawaldeh, A.A., 2023. The Efficiency of Using Machine Learning Techniques in Fiber-Reinforced-Polymer Applications in StructuralEngineering. *Sustainability*, *16*(1), pp. 11.

[21] [17] Kumar, M., Saini, J.S. and Bhunia, H., 2023. Radiation Curing of Fiber Reinforced Polymer Composite Based Mechanical Joints. In *Applications of High Energy Radiations: Synthesis and Processing of Polymeric Materials* (pp. 107-148). Singapore: Springer Nature Singapore.

[22] [18] Chauhan, S., Singh, M. and Kumar Aggarwal, A., 2021. An effective health indicator for bearing using corrected conditional entropy through diversity-driven multi-parent evolutionary algorithm. *Structural Health Monitoring*, *20*(5), pp. 2525-2539.

[23] [19] Kumar, A. and Kumar, R., 2017. Time-frequency analysis and support vector machine in automatic detection of defect

from vibration signal of centrifugal pump. *Measurement*, *108*, pp. 119-133.

[24] Kumar, M., Saini, J.S., Bhunia, H. and Chowdhury, S.R., 2021. Aging of bolted joints prepared from electron-beam-cured multiwalled carbon nanotube-based nanocomposites with variable torques. *Polymer Composites*, *42*(8), pp. 4082-4104.

[25] Kumar, M., Saini, J.S. and Bhunia, H., 2021. Investigations on MWCNT embedded carbon/epoxy composite joints subjected to hygrothermal aging under bolt preloads. *Fibers and Polymers*, *22*(7), pp.1957-1975.